Case Studies in Construction Materials 16 (2022) e01061

Contents lists available at ScienceDirect

Case Studies in Construction Materials

journal homepage: www.elsevier.com/locate/cscm

Case study

Optimizing the concrete strength of lightweight concrete containing nano palm oil fuel ash and palm oil clinker using response surface method

Hussein M. Hamada [a,*], Alyaa A. Al-Attar [b], Bassam Tayeh [c], Fadzil Bin Mat Yahaya [a]

[a] Faculty of Engineering Technology, University Malaysia Pahang, 26300 Pahang, Malaysia
[b] Northern Technical University, Mosul, Iraq
[c] Faculty of Engineering, Islamic Gaza University, Gaza, Palestine

ARTICLE INFO

Keywords:
Lightweight aggregate concrete
Palm oil clinker
Palm oil fuel ash
Nano-POFA
Flexural and splitting tensile strengths
Response surface method

ABSTRACT

Lightweight aggregate concrete (LWAC) has gradually gained popularity as a significant material in the concrete industry worldwide. One of the important lightweight aggregates is palm oil clinker (POC). Moreover, palm oil fuel ash (POFA) can be used as a partial cement replacement in concrete. This paper presents a study in which POFA of Nano-particle size was used to enhance the lower performance of LWAC made with POC aggregate. The Nano-POFA (NPOFA) was used as cement replacement of 0%, 10%, 20%, and 30% and POC aggregate was used as coarse aggregate at replacement levels of 0%, 50%, and 100%. Flexural and split tensile strengths and ultrasonic pulse velocity (UPV) were investigated for different concrete mixtures. For optimizing the parameters of the mix design, the response surface method (RSM) was adopted, and within it, a central composite design (CCD) approach was used. The results show that the interaction of POC and NPOFA affects the responses (UPV, flexural and tensile strengths). However, the POC tends to decrease all the responses. Whereas, the NPOFA tends to increase it especially at later ages. The highest UPV, flexural and split tensile strengths were observed for mixture (M7) that were 4375 m/s, 8.53 MPa, and 5.38 MPa, respectively. It can be concluded that the optimization method by RSM is an active way to enhance the mix design of LWAC.

1. Introduction

The economic advantages of palm oil industry have led to the expansion of the plantation area of oil palm trees worldwide from 6 to 16 Million hectares between 1990 and 2010 [1]. Malaysia and Indonesia are the two largest countries in the world that grow oil palm trees [2–4]. It was reported that in 2019 the biggest oil palm plantation was in Indonesia covering 2,424,545 ha [5]. Zaini et al. [6] reported that each hectare of land commonly housed about 135 oil palm trees. The increased plantation area of oil palm trees has caused the solid waste generated by palm oil production in the palm oil mills increase as well. These waste materials including kernels, empty fruit bunches, fibers, and oil palm shells are commonly dumped into landfills, which causes environmental issues [7,8]. At the same time, owing to the lack of availability of lightweight aggregate in most countries, the use of solid waste produced by palm oil mills, such as palm oil clinker (POC), is becoming increasingly beneficial as an alternate lightweight aggregate [9,10].

* Corresponding author.
E-mail address: enghu76@gmail.com (H.M. Hamada).

https://doi.org/10.1016/j.cscm.2022.e01061
Received 26 February 2022; Received in revised form 4 April 2022; Accepted 7 April 2022
Available online 11 April 2022

Approximately a ton of harmful CO_2 gas is generated while producing a ton of cement [11,12]. Also, about 7% of the undesired gases released into the atmosphere are due to the production of cement [13]. To address this problem, researchers have adopted various supplementary cementitious materials (SCM) as alternatives to the ordinary Portland cement (OPC), such as, palm oil fuel ash (POFA) [14–16], fly ash (FA) [17,18], silica fume (SF) [19,20], and ground-granulated blast-furnace slag (GGBFS) [21–23]. These materials have excellent pozzolanic reactions [24,25]. Numerous previous studies have reported that the use of SCMs is an effective step to achieve a sustainable construction industry [26,27]. One of these SCMs is POFA, which is a waste by-product from the palm oil industry [28,29].

In 2007, Malaysia alone produced about three million tons of POFA [30]. Large amounts of POFA are usually disposed into landfills without a suitable treatment, which causes health hazards and environmental issues [31,32]. Therefore, many researchers have investigated POFA as high pozzolanic material to replace cement in different proportions [33,34]. However, the large-sized particles of raw-POFA give it a weaker microstructure making it less efficient compared to ground POFA (GPOFA) [35]. Consequently, the GPOFA has been used as cement replacement by some researchers due to its better microstructure and higher pozzolanic reactions [30]. Besides, POFA has a high content (up to 67%) of silicon dioxide (SiO_2) [36], which enables it to easily react with calcium hydroxide (CH) to produce extra calcium-silicate-hydrate (*C-S-H*) gels [37,38]. Therefore, the pozzolanic reaction of POFA can enhance the concrete strength and microstructure properties, particularly at later age [15,39,40]. Most of the researchers investigating the use of POFA at different replacement levels have concluded that the concrete performance remains acceptable with the replacement levels up to 30% [4,41]. Exposing the POFA particles to extra grinding leads to improving the pozzolanic reactions, thus increasing the resulting concrete strength [42]. Some researchers have utilized Nano-sized POFA to examine the microstructure properties and hydration-temperature of the resulting mortar [40,43]. However, there are not many studies using Nano POFA (NPOFA) aimed at finding out the resulting concrete strength [37,43,44]. The effects of NPOFA on the properties of concrete need to be studied lengthily. Due to the pozzolanic reaction between high volume of ground PFOA and calcium hydroxide (CaOH) released from hydration of cement, the strength of concrete with 20% POFA was somewhat higher than that of ordinary cement concrete [45]. The pozzolanic reaction of the GPOFA in cement mortar increased, especially with later ages [39]. The compressive strength of blended cement paste is higher than that of the ordinary cement paste due to increase in pozzolanic reaction at later ages [46].

The preciousness of natural aggregates has compelled many researchers to utilize oil palm shell (OPS) and palm oil clinker (POC) to fulfill the increasing demand for suitable aggregates in the concrete mixtures [47]. Palm oil mills generate large quantities of POC as a waste byproduct [48]. The use of POC as lightweight aggregate (LWA) can produce lightweight concrete (LWAC) with satisfactory strength [48]. The use of POC as coarse aggregate reduces the construction cost and minimizes the environmental issues related to the accumulation of these wastes. In addition, the LWAC has many advantages such as the reduction in dead load, diminishing of micro-cracks, and uniform stress distribution [49,50]. Numerous studies have been conducted to show the effects of POC as coarse aggregate on the concrete performance. Kabir et al. [51] investigated the influence of incorporating different replacement levels of POC as coarse aggregate with GGBS and POFA to make geopolymer concrete (GPC). It is an aggregate with high pozzolanic reaction properties and high bonding potential in the LWAC mixture owing to containing aluminosilicates in their composites. Hamada et al. [37] utilized POC as a coarse aggregate in the production of LWAC. POC was used in different replacement levels of 0%, 50%, and 100%, while NPOFA was used to replace cement at different replacement levels of 0%, 10%, 20%, and 30%. They observed that the highest compressive strength was 58.3 MPa resulting from the concrete mix containing 30% NPOFA and 0% POC, whereas, the lowest value for the same was 40.7 MPa. These results point to the high effects of NPOFA on the concrete strength. Therefore, this paper presents a study in which POFA of Nano-particle size was used to enhance the lower performance of LWAC made with POC aggregate. The Nano-POFA (NPOFA) was used as cement replacement of 0%, 10%, 20%, and 30% and POC aggregate was used as coarse aggregate at replacement levels of 0%, 50%, and 100%. This paper also reports the results of a research on the UPV, flexural and splitting tensile strengths of LWAC containing POC as partial/full coarse aggregate replacement and NPOFA as partial cement replacement. A total of thirteen concrete mixtures have been designed using the response surface method (RSM), including one control

Table 1
Physical and chemical properties of the binder materials.

Properties	Cement	NPOFA
Calcium oxide (CaO)	53.8	3.97
Silicon dioxide (SiO_2)	26.1	67.3
Aluminum oxide(Al_2O_3)	8.54	4.12
Ferric oxide(Fe_2O_3)	4.09	8.12
Sodium oxide (Na_2O)	0.186	0.115
Titanium oxide (TiO_2)	0.427	0.229
Magnesium oxide (MgO)	0.358	2.72
Potassium oxide (K_2O)	0.97	8.45
Manganese oxide (MnO)	0.137	0.07
Phosphorus pentoxide (P_2O_5)	0.177	2.47
Sulfur trioxide (SO_3)	2.77	0.535
Loss of Ignition (LOI)	2.2	1.4
Specific gravity	3.15	2.52
Mean particle size (μm)	6.8	0.982
Blaine Fineness (cm^2/g)	3310	4830
Specific surface area (m^2/g)	0.782	1.962

Fig. 1. (A) Raw-POFA (B) Ground-POFA (C) Nano-POFA.

mix.

2. Materials and methodology

2.1. Materials

2.1.1. Binder materials

The ordinary Portland cement (OPC) was used as the primary binder material. NPOFA has been used to partially replace OPC. The chemical composition and physical properties of the binder materials were studied in the chemical laboratory at University Malaysia Pahang, which are listed in Table 1. Palm oil fuel ash (POFA) was collected in the required quantity for experimental tests from a local (Pahang, Malaysia) palm oil mill. The collected POFA was subjected to many treatment processes including drying the collected sample in an electric oven at $110 \pm 10^{o}C$ for a day. The treatment processes were explained in detail elsewhere by Hamada et al. [37]. The final product was Nano-POFA. A sample of POFA exposed to the different treatment processes has been shown in Fig. 1.

2.1.2. Coarse aggregates

Palm oil clinker (POC), a by-product material generated from the palm oil mills as waste material in large chunks, was used as partial replacement of the natural coarse aggregates. The required quantity of POC was sourced from a nearby palm oil mill. Many steps of treatments were performed in the concrete laboratory on the raw POC collected, as shown in Fig. 2. Firstly, the raw POC was washed to remove any dust and other organic materials, and then dried in an electrical oven at $110 \pm 10^{o}C$ for a day. Secondly, large chunks of POC were crushed to obtain smaller pieces. Lastly, the sieving analysis was conducted to separate the fine and coarse aggregate sized pieces.

The same treatment steps were conducted previously by Ahmmad et al. [48]. The resulting aggregates have lower density than natural aggregate and can be considered as LWA [52]. POC aggregate has low bulk density and high water absorption. Its weight is 49% lower than the conventional coarse aggregates [53] and 29% lower than the conventional fine aggregates [54]. Therefore, the use of this LWA is expected to decrease the structural dead load and consequently reduce the total construction cost by a significant amount. The comparison of the properties, such as the aggregate impact value (AIV) and the aggregate crushing value (ACV) of POC aggregates, which are higher than those of the natural aggregate [54], and mining sand was used as fine aggregate with the properties as listed in Table 2. Fig. 3 shows the gradation of the particle size of the crushed stone and the POC coarse aggregates used to prepare the specimens.

2.2. Microstructure properties of POFA

The Scanning electron microscope (SEM) test was carried out to identify the variations in POFA morphologies. POFA was treated through numerous procedures starting with oven-drying raw POFA in an electrical oven at $110 \pm 10^{o}C$ for 24 h followed by grinding to obtain GPOFA. Los Angeles machine was used for the grinding. The GPOFA was heated in an electrical furnace at a temperature of up to $600^{o}C$ for 2 h to get the treated POFA (TPOFA). The TPOFA was ground again to get ultrafine POFA (UPOFA). The results of SEM/EDX of GPOFA show that the particle shape was irregular and angular with a porous texture. After the heating of GPOFA, no agglomeration of POFA was noted. The shape and size of TPOFA was somehow similar to the GPOFA except some variations, however, its carbon content was lower owing to the exposure of TPOFA to heat-treatment which burned excess carbon. The particle size of UPOFA was less than that of GPOFA and TPOFA particles and the shape was generally semi-circular and usually angular. The SEM/EDX of various POFA morphologies are shown in Figs. 4–6.

On the other hand, the EDX test was used to get the information on the chemical composition of various POFA morphologies. Changes in the mechanical properties and chemical composition can be attributed to the various treatment procedures. The specific surface area and particle size of UPOFA particles were determined as being only 1.962 m^2/g and 0.982 μm, respectively. This shows

Fig. 2. Processing of POC aggregate.

Table 2
Physical properties of natural fine and coarse aggregates and POC.

Properties	Natural fine aggregates	Natural coarse aggregate	POC coarse aggregate
Aggregate size (mm)	0.3–4.75	4.75–10	4.75–10
Bulk density (kg/m3)	2.79	1452	732
Fineness			6.23
Specific gravity (SSD)	2.64	2.65	1.78
Water absorption (24 h) %	0.82	0.74	5.7
Moisture content %		0.29	0.38
Los Angeles abrasion value (%)		23.9	49.7
Aggregate impact value (AIV)%			31.57
Aggregate crushing value (ACV)%		16.8	46.5

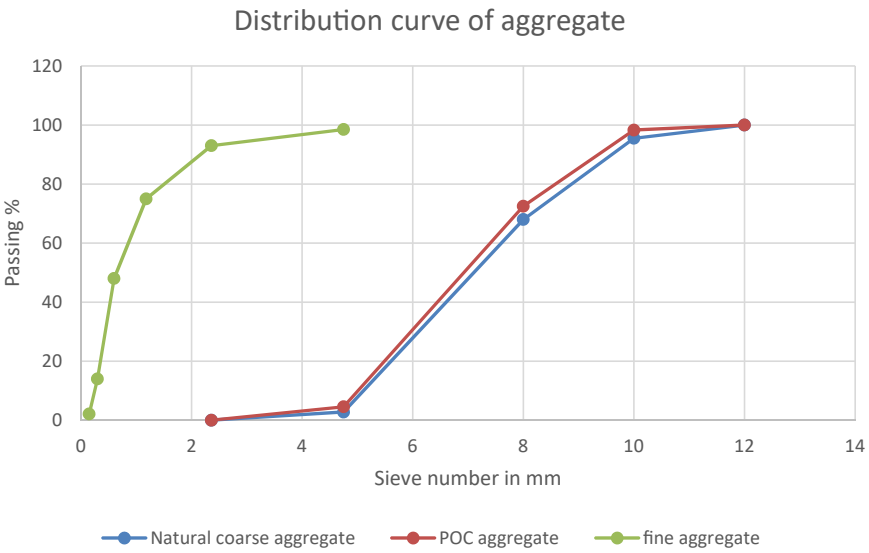

Fig. 3. Sieve analysis of aggregates used.

that UPOFA has a smaller particle size resulting in a higher surface area than that of both the raw POFA and cement. On the other hand, the carbon content reduced as identified by the SEM/EDX test. Therefore, due to the reduced carbon content and loss of ignition (LOI), the SiO_2 content in UPOFA increased in comparison to the raw POFA and GPOFA. The heat treatment process also caused an increase in the content of Fe_2O_3 and Al_2O_3. Consequently, according to the requirements of ASTM C618, the UPOFA can be classified as a mineral admixture class F. The SEM/EDX tests have also illustrated the color changes of TPOFA and UPOFA due to the exposure to the heating process and further grinding. The decrease of carbon content in UPOFA particles led to a substantial variation in the color from black to reddish-gray.

2.3. Microstructure analysis of POC aggregate

Assessment of the microstructure of POC is significant in order to assess the material's performance in the concrete mix. The scanning electron microscopy (SEM) exams were performed to outline the microstructural properties of POC, while the energy dispersive X-ray (EDX) was utilized to chart its chemical composition. Fig. 7 shows the presence of a large amount of voids spread across the POC surface. These micro voids may cause a crack on the concrete surface especially when connected with each other, thus reducing the concrete strength.

2.4. Mixing procedure and test methods

For sample preparation, the mining sand and POC aggregate were initially mixed in a drum mixer for a duration of 5 min. The binder materials (NPOFA and cement) were then added according to the proportion designed beforehand and the mixing was done for an additional 3 min. Water was added gradually along with superplasticizer and the mixing continued for 5 min when a uniform concrete mix consistency ensued. After the mixing process, a vibration table was used to compact the concrete in molds for 30 s. The samples were demolded after 24 h from casting time. All concrete samples were cured under water until the test day. The humidity and ambient temperature of the laboratory were about 76% and $27 \pm 3^{o}C$, respectively. Consistent humidity and temperature were due to the prevailing climatic conditions in Malaysia. The experimental tests included the compressive strength, ultrasonic pulse velocity,

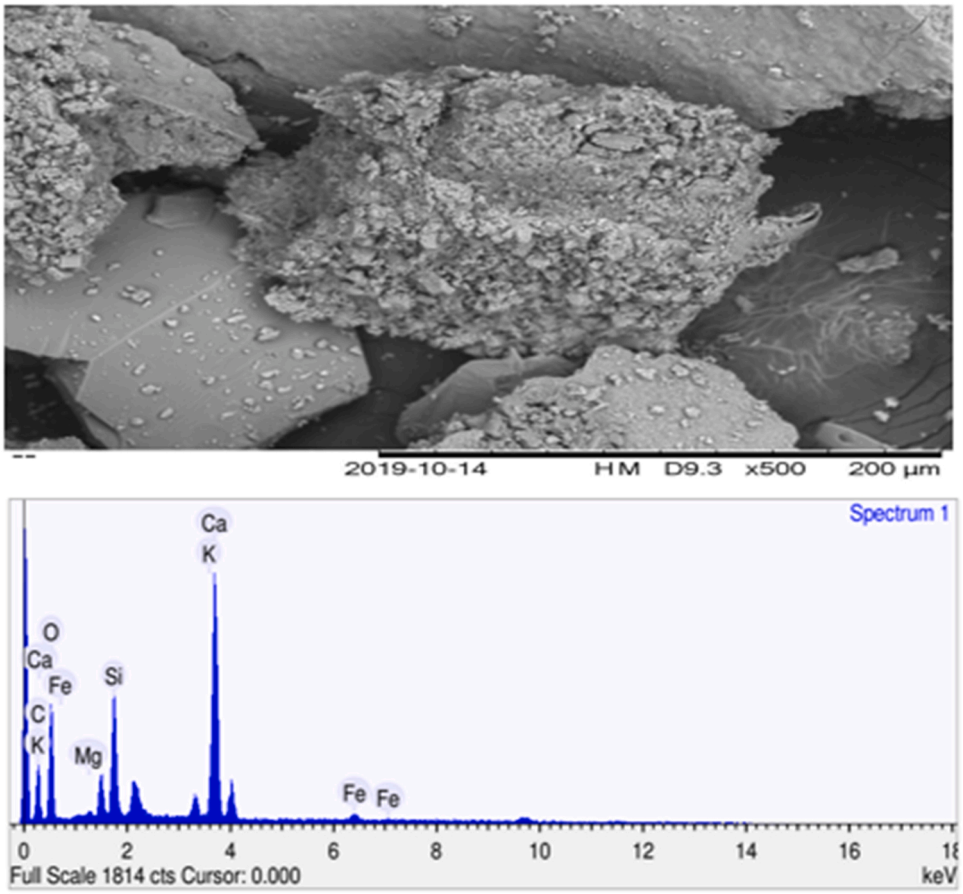

Fig. 4. SEM/EDX of GPOFA.

flexural and splitting tensile strength. The flexural and splitting tensile strengths and compressive tests were conducted respectively on prism, cylindrical and cubic samples in accordance with BS-1881-Part-117. The non-destructive test (UPV) were conducted based on ASTM C597.

2.5. Mix design using response surface method

Response surface methodology (RSM) connects the outputs with autonomous variables to find out the effect of an association between autonomous factors and dependent variables (responses) [55]. RSM is being utilized in many research areas to produce models required including the concrete mixtures design [56]. A central composite design (CCD) is used in RSM [55]. It was credited as a possibly suitable method which is capable of offering appropriate functional association between the independent variables (factors) and responses [57]. Design Expert v12 software was used in this study for the design and statistical analysis. It was also used to optimize the responses. Analysis of variance (ANOVA) was performed to detect any correlation between the different factors and the effect of each factor. A suitable regression model was used, as illustrated in the Eq. (1) [55,58]:

$$Y = \beta_o + \sum_{i=1}^{k} \beta_i x_i + \left(\sum_{i=1}^{k} \beta_{ii} x_i \right) + \sum_{i=1}^{k-1} \sum_{j}^{n} \beta_{ij} x_i x_j + e \quad (1)$$

where, Y is the response, x_i and x_j are the variables, k is the number of parameters included in the experiment, β is the regression coefficient, and e is the random error.

Table 3 illustrates the level and the ranges of all the variables (factors, namely POC and NPOFA) investigated. Thirteen experimental tests were conducted ($2^k + 2k + 5$), where k is the number of variables (k = 2). Eight various combinations were complemented with the addition of five replicates of the medium-case.

The tests were required to find out the proficiency of NPOFA as a partial cement replacement and POC as partial/full replacement of coarse aggregate on the concrete strength. Thirteen experimental tests were implemented according to the central composite design (CCD) as given in Table 4. The relationship between the two factors NPOFA% and POC% and the three responses (UPV, flexural and splitting tensile strengths) were investigated using RSM. The expected results (*Y*) were calculated to evaluate the factors as a function

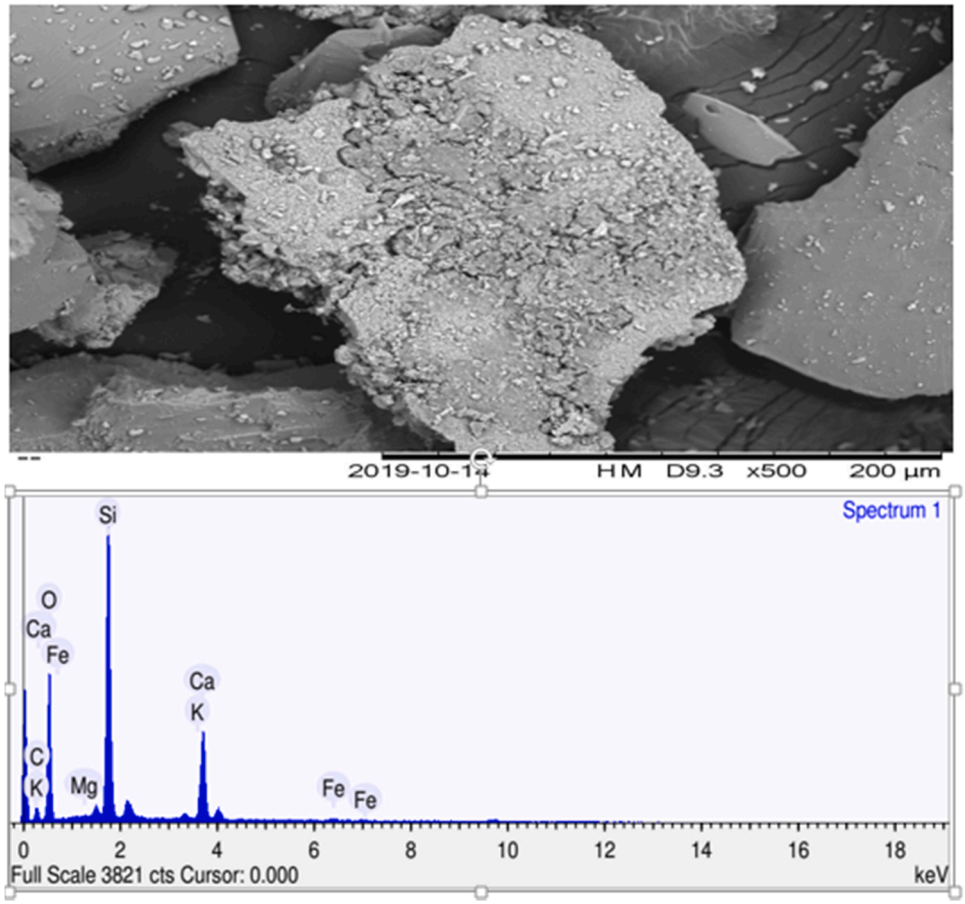

Fig. 5. SEM/EDX of TPOFA.

of x_1 (NPOFA)% and x_2 (POC)%.

3. Experimental results and discussions

3.1. Ultrasonic pulse velocity (UPV)

The ultrasonic pulse velocity (UPV) is a significant test carried out to determine the concrete quality and consistency as well as to find out the presence of cracks and voids. Using the testing standard ASTM C597–16, the UPV test was conducted on 100-mm cubic samples at the ages of 7, 28, 90, 180, and 360 curing days for all concrete mixes as shown in Fig. 8. The samples were classified as very poor, poor, good, very good, and excellent for the corresponding UPV values of less than 2.0, 2–3, 3–3.5, 3.5–4.5, and more than 4.5 km/s, respectively; according to Whitehurst [59]. Generally, the LWAC produces lower UPV values than normal concrete [60]. The results show that the mix M4 with 100% POC aggregate and 30% UPOFA as cement replacement achieved the lowest UPV value of 3.212 km/s at 360 days, which still falls in the range between 3.0 and 3.5 km/s and can be classified as "good" quality. This low UPV value can be attributed to the porosity of POC aggregate. The lack of interlocking between aggregates generates voids and that results in a lower UPV travel rate. Nevertheless, the remaining concrete mixtures were located between "good" and "very good" quality as those ranged 3.0–3.5 and 3.5–4.5 km/s.

On the other hand, Awal et al. [61] reported that the addition of POFA into the concrete mixtures as cement replacement has a positive effect on the UPV value. Another study by Awal et al. [62] reported that higher temperature led to lower UPV values. The UPV at an initial temperature of 27^oC was 4539 m/s, but reduced at higher temperatures to be ranging between 3655 and 4117 m/s for concrete containing POFA at all replacement levels. Islam et al. [38] reported that 5–15% POFA replacement level of cement is the optimum to achieve high UPV values whereas an increase in the POFA quantity lead to a decrease in the UPV values, especially with more than 20% replacement level.

Abutaha et al. [63] reported that the irregular nature and high porosity of POC aggregate affects the wave propagation across concrete samples. The presence of empty voids between and within the aggregate decreases the pulse velocity particularly with a high POC content in concrete mixtures. Jumaat et al. [64] concluded that the UPV values of the mixtures containing 75% and 100% POC

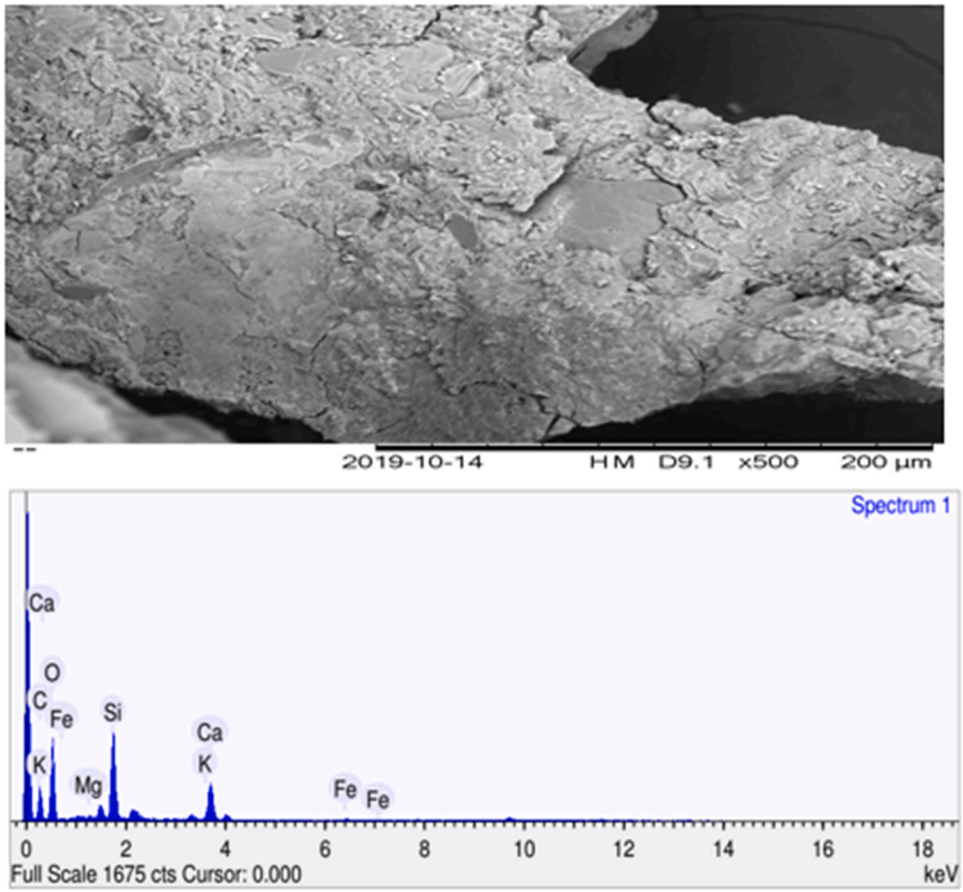

Fig. 6. SEM/EDX of UPOFA.

indicated that it is "good" concrete after exposure to $500^{o}C$ for an hour [65]. Kanadasan et al. [66] used the different replacement levels of POC to produce self-compacting concrete (SCC). They reported that even though the UPV values decreased, yet the POC concrete was still in the category of "good" concrete and contributed to a significant reduction in cost and energy utilized. Abutaha et al. [67] stated that the UPV values of LWAC containing POC were in "very good" category for all replacement levels. This may be due to using silica fumes and POC powder in the blending materials. Other study conducted by Hamada et al., [37] proved that the lower UPV values are due to the increment of POC content, which results in raised air content in the UHPC samples.

3.2. Flexural strength

Four-point bending test was carried out to measure flexural strength according to ASTM: C1018–97 [68]. It can be noted that the flexural strength of mix M7 (0% POC, 15% NPOFA) is the highest among all the concrete mixtures at 8.53 MPa at 360-days as shown in Fig. 9. Whereas, the lowest flexural strength at 360 days was that of M4 (100% POC, 30% NPOFA) at 5.05 MPa. Cracks started appearing at the weaker part in the interfacial zone (IZ) followed by the flexural failure. The flexural strength in the mix M7 was about 9% more than the control concrete M1 that achieved 7.82 MPa at 360 days. While Mix 4 including 30% NPOFA and 100% POC was about 35% lower than the control mix. The decrease in the flexural strength can be attributed to the sharp and angular edges of POC, which when mixed with binders caused stress concentration of concrete cracks and reduced the resistance to crack growth. Ahmad et al. [69] reported similar results. Alengaram et al. [70] reported that utilization of high volume of foam can produce large quantity of air content in the mix that decreases the strength and density of concrete.

The flexural strength of the control concrete specimen increased from 6.65 MPa at 28 days to be 7.82 MPa at 360 days, with an increase of 17.6%. Whereas, the increase in the flexural strength of the mix M4 was about 25% from 28-days (4.05 MPa) to 360-days (5.05 MPa). This indicates that the control sample achieved about 82% of its total flexural strength in the first 28 days, whereas the mix M4 achieved only 75% of its total flexural strength during that time. Therefore, M4 mix exhibited a slower rate flexural-strength-gain than the control sample.

Mohammadhosseini et al. [71] investigated the feasibility of utilizing POFA with waste metalized plastic (WMP) fibers in concrete to enhance the mechanical properties. The mixture of POFA and WMP fibers enhanced the flexural and tensile strengths when POFA was used as cement replacement up to 20%. The enhancement in the POFA mixtures was attributed to the higher reactivity of POFA at

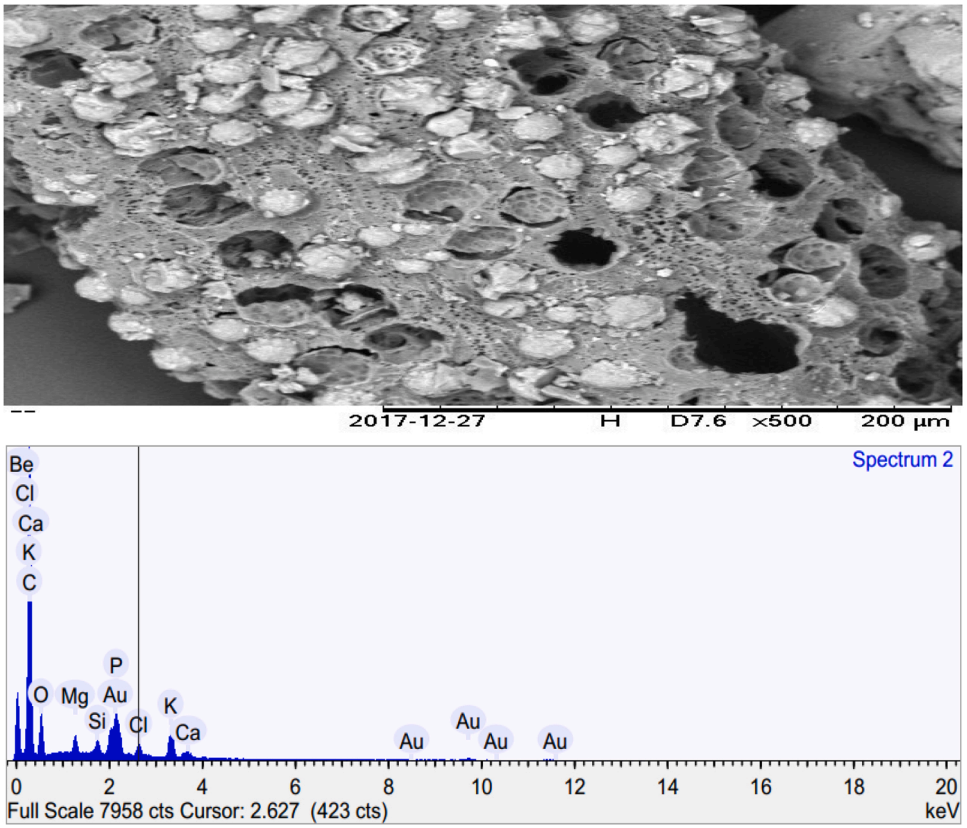

Fig. 7. SEM/EDX of the POC aggregate.

Table 3
Variables investigated with units and coding values.

Variables (factors)	Code	Unit	-1	0	1
NPOFA	A	%	0	15	30
POC	B	%	0	50	100

Table 4
CCD model by RSM technique.

Mix no.	NPOFA %	POC %	NPOFA Kg/ m^3	Cement Kg/ m^3	POC Kg/ m^3	Coarse aggregate kg/m^3	Fine aggregate Kg/m^3	Water/ binder	superplasticizer %
1	0	0	0	450	0	900	700	0.42	1
2	30	0	108	315	0	900	700	0.42	1
3	0	100	0	450	604	0	700	0.42	1
4	30	100	108	315	604	0	700	0.42	1
5	0	50	0	450	302	450	700	0.42	1
6	30	50	108	315	302	450	700	0.42	1
7	15	0	54	382.5	0	900	700	0.42	1
8	15	100	54	382.5	604	0	700	0.42	1
9	15	50	54	382.5	302	450	700	0.42	1
10	15	50	54	382.5	302	450	700	0.42	1
11	15	50	54	382.5	302	450	700	0.42	1
12	15	50	54	382.5	302	450	700	0.42	1
13	15	50	54	382.5	302	450	700	0.42	1

later curing times thus making further C-S-H gels which increase the concrete strength. Bashar et al. [72] reported that the use of steel fibers with high-volume POFA can improve the flexural strength and this could be owing to the capability of fibers to delay crack diffusion in concrete. Lim et al. [73] stated that the use of 10–20% POFA as a filler can increase higher flexural strength at all the curing

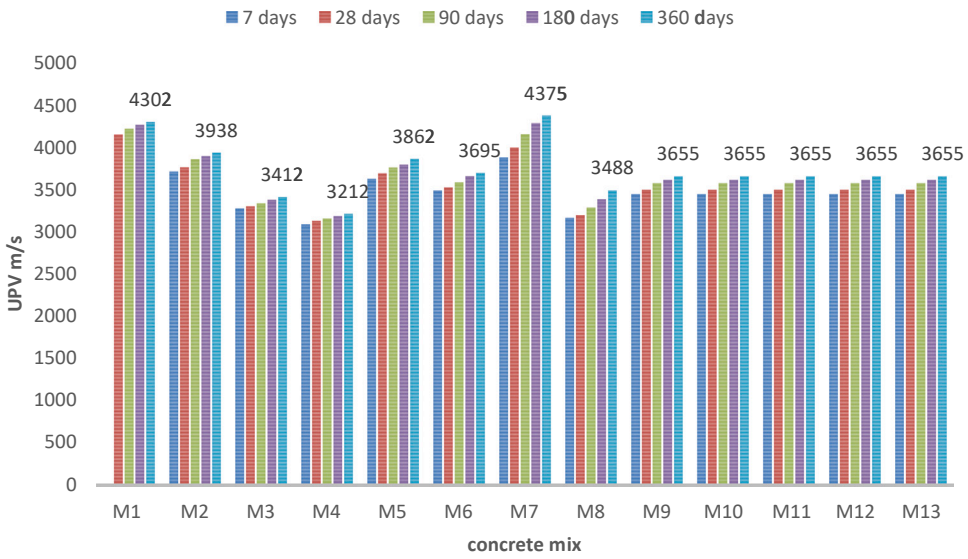

Fig. 8. UPV values of LWAC at different curing ages.

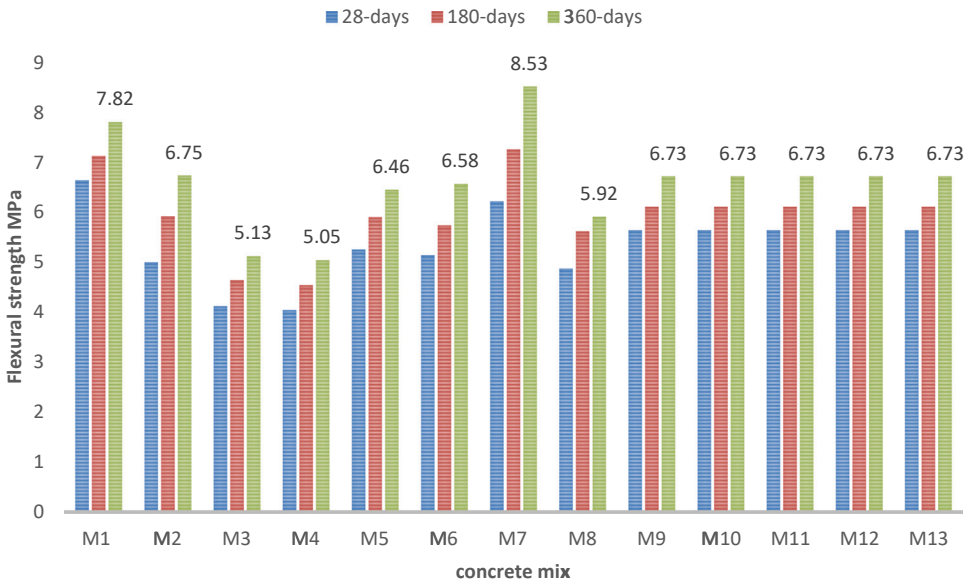

Fig. 9. Results of flexural strength test.

ages. Aldahdooh et al. [74] used the RSM method to predict the flexural and tensile strength of ultra-high performance fiber reinforced cementitious composites containing 75% of ultrafine palm oil fuel ash (UPOFA). They observed that utilizing UPOFA as cement can enhance the concrete strength.

The flexural strength decreased by about 17% due to early cracks in the POC concrete samples in the study by Nayaka et al. [75]. They used 50% palm oil clinker powder (POCP) as a binder and up to 100% POC as coarse aggregate. They reported that the optimal mix design of 30% POCP and 50% POC achieved 83% of flexural strength as compared to the control. Aslam et al. [76] stated that the POC concrete exhibited 26% higher flexural strength at 28-days compared to its 7-day strength. However, the POC concrete samples showed a similar flexural strength and flexural/compressive strength ratio to normal weight concrete (NWC) and high strength-LWAC. Muthusamy et al. [77] studied the long-term mechanical properties of high strength POC concrete containing 10–40% GPOFA as cement replacement. The application of 10% GPOFA enhanced the flexural strength significantly compared to other mixtures including the control specimen. Abutaha et al. [67] stated that the POC aggregate has a negative influence on the flexural strength values when they observed a significant reduction (up to 39% compared to the control) in the flexural strength.

3.3. Splitting tensile strength

The Splitting tensile strength test was used to evaluate the susceptibility of concrete to cracking. The casting of concrete mixtures was done in cylindrical molds. The test was carried out for 28, 180, and 360 days as illustrated in Fig. 10 which shows that Mix 7 with 0% POC and 15% NPOFA achieved the highest tensile strength of 5.38 MPa at 360 days, which was slightly higher than the control concrete specimen, only by 4.65%. Whereas, the lowest tensile strength was that of M4 (100% POC and 30% NPOFA), which achieved 2.90 MPa at 28-days and 3.45 MPa at 360-days, less than the control concrete specimen by 32.75%. The decrease in splitting tensile strength of 100% POC aggregates is due to have porous appearances which assist to develop the micro cracks at testing time and result to decrease the strength value, the similar reason was stated by Polat et al. [78].

The splitting tensile strength of the control concrete specimen increased from 4.72 MPa at 28 days to be 5.13 MPa at 360 days, with an increase of 8.7%. Whereas, the increase in the splitting tensile strength of the mix M4 was about 19% from 28-days (2.9 MPa) to 360-days (3.45 MPa). This indicates that the control sample achieved about 91% of its total splitting tensile strength in the first 28 days, whereas the mix M4 achieved only 81% of its total splitting tensile strength during that time. Therefore, M4 mix exhibited a slower rate splitting-tensile-strength-gain than the control sample.

As can be seen in Fig. 10, the highest splitting tensile strength was recorded in mix 7 containing 15% NPOFA and 0% POC. It's the same mix that recorded the highest values for both the UPV and flexural strength. While, the lowest splitting tensile strength was recorded for mix 4 containing 30% NPOFA and 100% POC at all curing ages. These results are similar to the study conducted by Hassan et al. [79], who reported that the higher tensile strength was noted for their mixes 1, 2, and 3, which contained 1–3% nano POFA with 10% micro POFA at both the early and later ages. The highest value of the splitting tensile strength was due to the addition of nano-POFA that increased the pozzolanic reactivity and improved the pore-refinement of the concrete mix. Islam et al. [38] reported that the addition of POFA up to 25% did not significantly influence the concrete properties, whereas the use of 10–15% POFA as cement replacement enhanced the concrete strength.

Regarding the effect of POC on the splitting tensile strength, Abutaha et al. [67] reported that the replacement of normal coarse aggregate with POC resulted in a loss of splitting tensile strength. Ahmmad et al. [80] used POC powder as cement replacement and POC as coarse aggregate to achieve a 28-day splitting tensile strength of more than 2.0 MPa, which is an acceptable value for structural purposes. On the other hand, the splitting tensile strength of concrete containing POC was reported to range between 3.05 and 3.31 MPa by Aslam et al. [9].

4. Mathematical modeling and statistical analysis

The experimental results were modeled using the software 'Design Expert' in order to determine the best fit polynomial function. Regression analysis was carried out to establish correlations between the independent variables and the experimental values obtained. To omit the statistically insignificant terms, t-statistics were used until the estimated model for each response became entirely significant. 95% confidence interval was used while performing the single factor ANOVA. Assuming normal distribution of the response, multiple regression analysis was used to calculate the coefficients of regression models as given in Table 5.

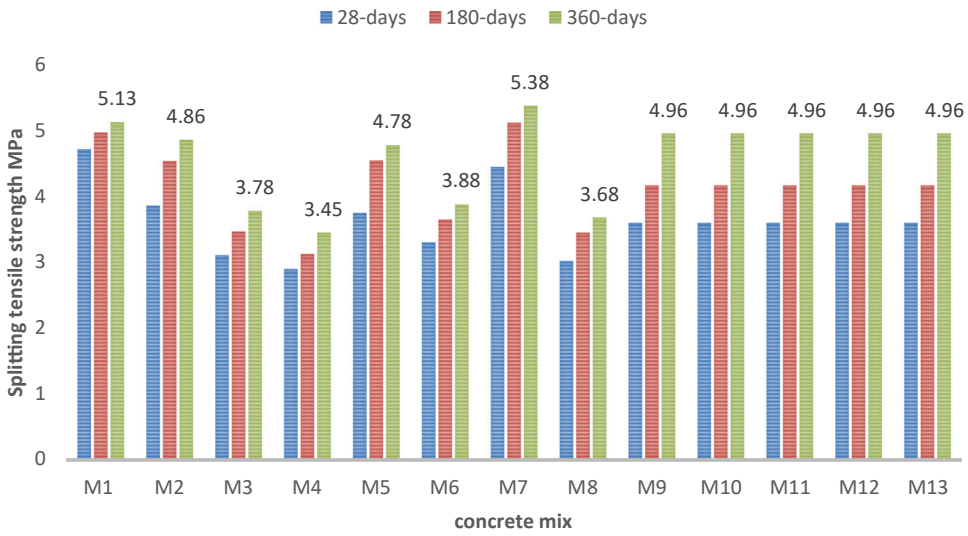

Fig. 10. Splitting tensile strength test results.

Table 5
ANOVA results for concrete responses.

Dependent variable	Source of variation	Sum of square	Df	Mean square	F	p-value	Status	R^2	Predicted R^2	Adjusted R^2	Adequate Precision
Ultrasonic pulse velocity	Model	1.133E+ 06	2	5.666E+ 05	44.38	< 0.0001	significant	0.8988	0.8284	0.8785	19.8607
	A-UPOFA	89,060.17	1	89,060.17	6.98	0.0247					
	B-POC	1.044E+ 06	1	1.044E+ 06	81.79	< 0.0001					
	Residual	1.277E+ 05	10	12,766.44							
	Lack of Fit	1.277E+ 05	6	21,277.41							
	Pure Error	0.0000	4	0.0000							
	Cor Total	1.261E+ 06	12								
Flexural strength	Model	9.67	5	1.93	19.61	0.0005	significant	0.9334	0.4749	0.8858	14.1457
	A-UPOFA	0.1768	1	0.1768	1.79	0.2225					
	B-POC	8.17	1	8.17	82.77	< 0.0001					
	AB	0.2450	1	0.2450	2.48	0.1591					
	A^2	1.03	1	1.03	10.40	0.0146					
	B^2	0.0252	1	0.0252	0.2554	0.6288					
	Residual	0.6907	7	0.0987							
	Lack of Fit	0.6907	3	0.2302							
	Pure Error	0.0000	4	0.0000							
	Cor Total	10.37	12								
Splitting tensile strength	Model	4.73	5	0.9459	24.78	0.0003	significant	0.9465	0.5316	0.9083	16.4688
	A-UPOFA	0.3750	1	0.3750	9.82	0.0165					
	B-POC	3.32	1	3.32	86.83	< 0.0001					
	AB	0.0009	1	0.0009	0.0236	0.8823					
	A^2	0.5214	1	0.5214	13.66	0.0077					
	B^2	0.1519	1	0.1519	3.98	0.0863					
	Residual	0.2673	7	0.0382							
	Lack of Fit	0.2673	3	0.0891							
	Pure Error	0.0000	4	0.0000							
	Cor Total	5.00	12								

4.1. Analysis of UPV test results

The UPV prediction model for a curing age of 360 days yielded a coefficient of determination of 0.898, indicating a very high precision. Between the two variables recorded in Table 5, the curve of the POC was much harsher than NPOFA, however, the NPOFA improved the concrete strength, especially at later ages, in comparison to the POC.

The combined effect of the NPOFA replacement level (%) (*A*) and POC replacement level (%) (*B*) on the UPV is illustrated by the perturbation plots in Fig. 11(a). It can be observed that the POC aggregate effect is harsher than NPOFA on the UPV value, which decreased from 4302 for the control mix to 3212 m/s for mix 4. The decrease in the UPV values can be attributed to the existence of voids and the pore structure of the POC surface. Whereas, the use of NPOFA up to 15% enhanced the UPV value of concrete to be higher than all the other concrete mixtures including the control, especially at later age. These trends have been observed with other responses also (flexural and splitting tensile strengths). The empirical relationship between the factors (NPOFA and POC) and the UPV in terms of coded factors as obtained from the UPV test results is presented in Eq. (2).

$$UPV = 3735.31 - 121.83A - 417.17B \quad (2)$$

The ANOVA values of response surface quadratic model for the UPV were shown in Table 5. The UPV model was significant because of the p-value ($P < 0.05$) with t-test at a 5% level of significance. The F-value of 44.38 with a low probability value shows that the model was significant. The ANOVA results illustrated a reliable confidence in the estimate of the UPV efficiency ($R^2 = 0.8988$). The predicted R^2 of 0.8284 agrees, within a reasonable limit, with the adjusted R^2 of 0.8785 for the UPV of LWAC. It is an acceptable adjustment as the value is high and close to 1. The adequate precision value of 19.8607 for the UPV, which is more than 4, is satisfactory and confirms the predicted model.

Fig. 11(b) shows the normal plots of the residual values of the UPV to assess the UPV and determine the model suitability. For the model adequacy, the residuals from the ANOVA results are significant. The plot between the studentized residuals and normal % of probability agreed with the straight line, hence, validating the model.

On the other hand, the effects of the NPOFA and POC replacement levels on the UPV of LWAC are validated in the 2D and 3D surface response plots as illustrated in Fig. 12. It can be observed in Fig. 12 that the low UPV values are related with a POC replacement level, when increase the POC as coarse aggregate, the UPV decreased to be 3212 m/s with 100% replacement level of POC and 30% UPOFA. While, the UPV with 15% NPOFA recorded of 4375 m/s.

4.2. Analysis of flexural strength test results

The combined effects of the NPOFA replacement level (%) (*A*) and POC replacement level (%) (*B*) on the flexural strength are described by the perturbation plots as illustrated in Fig. 13(a). The curvature (B) which represents the POC is certainly harsher than the curve (A), which shows that the flexural strength is more affected by the POC replacement level in the LWAC mix. The empirical

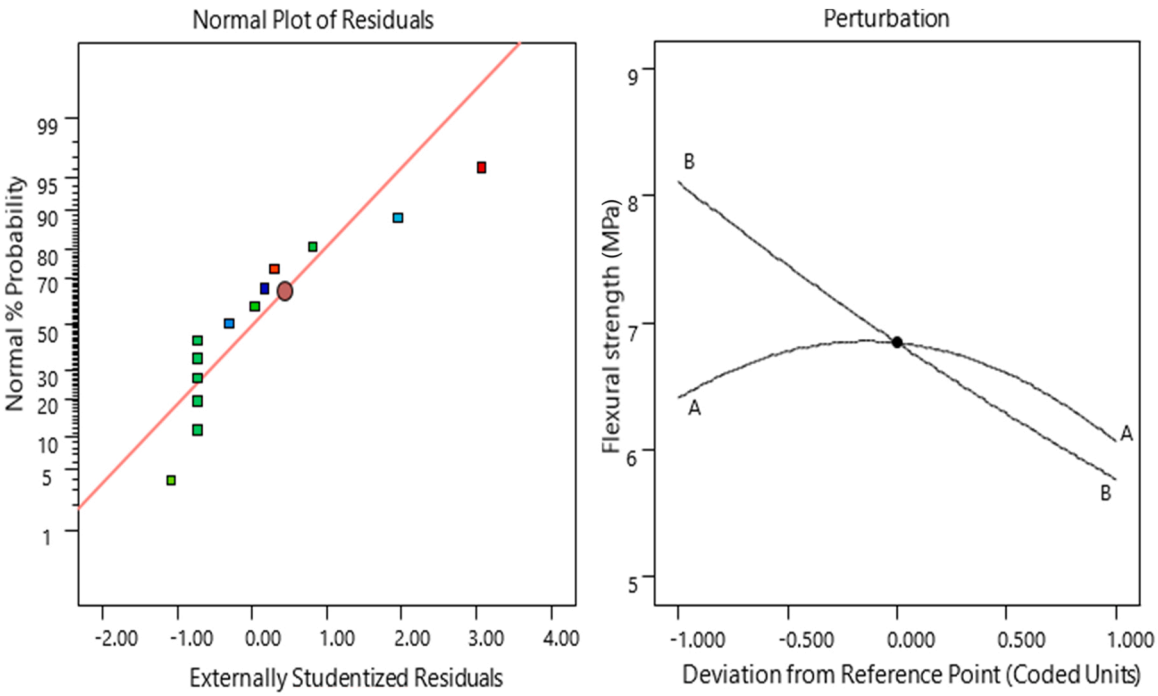

Fig. 11. Perturbation curve and Normal plots of the residual values of UPV test.

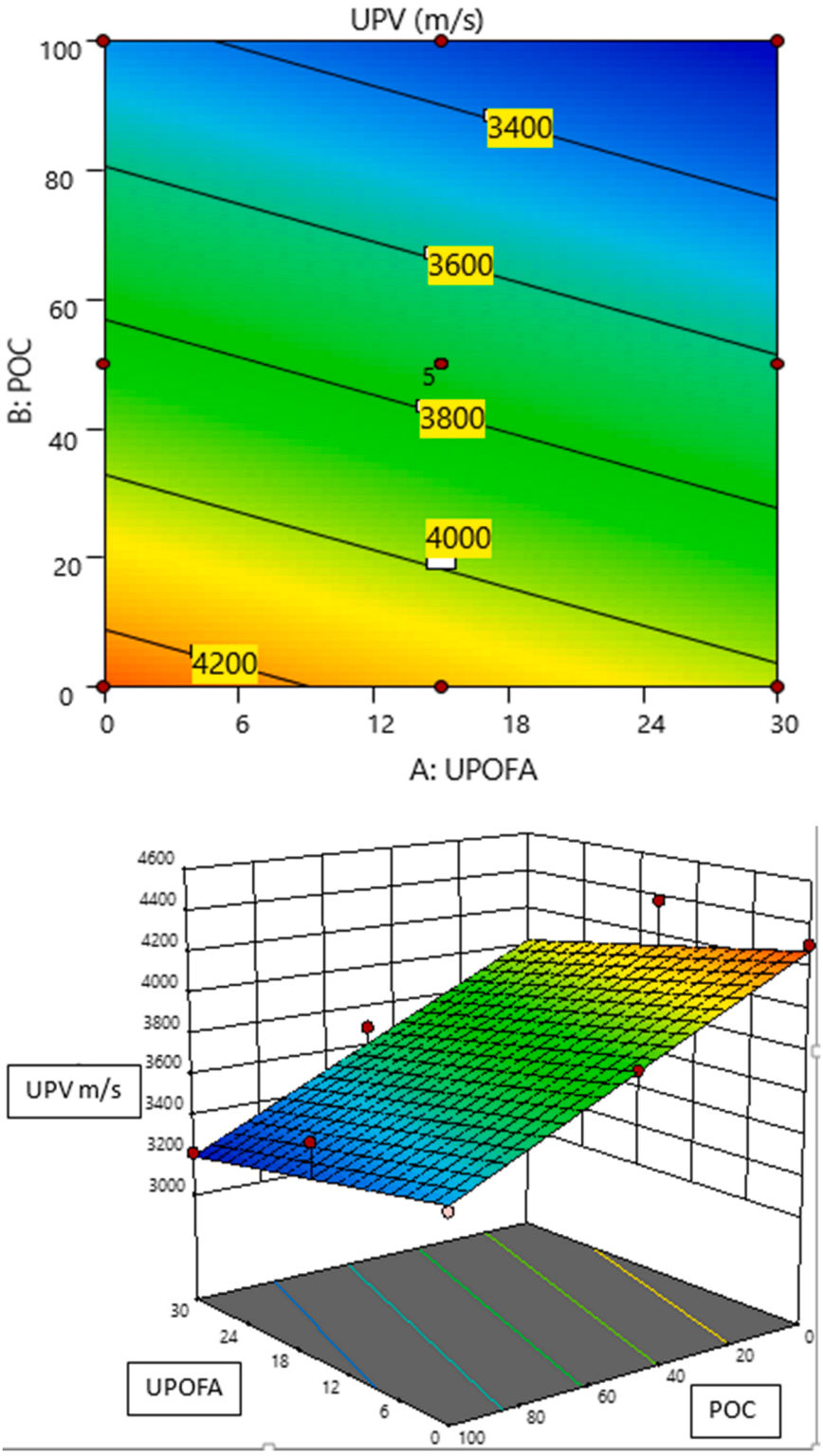

Fig. 12. 2D and 3D of UPV.

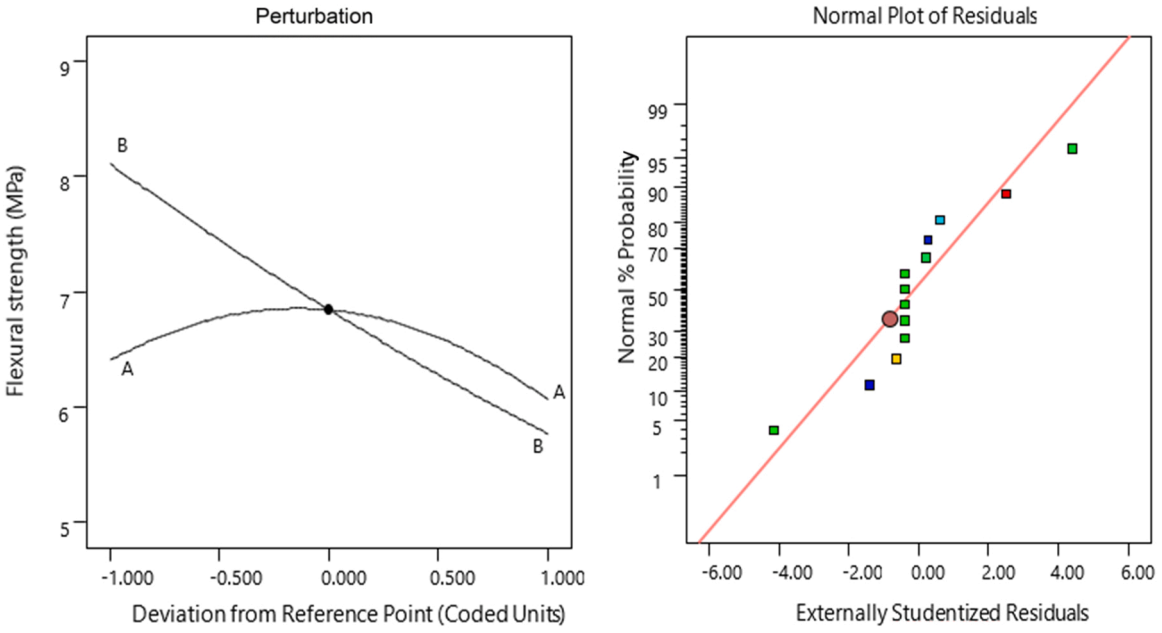

Fig. 13. Perturbation curves and normal plots of residual values of the flexural strength.

relationship between the factors (NPOFA and POC) and the flexural strength (σ) in terms of coded factors is given in Eq. (3).

$$\sigma = 6.84 - 0.1717A - 1.17B + 0.2475AB - 0.6095A^2 + 0.0955B^2 \quad (3)$$

The interaction between the factors significantly affected the flexural strength. The ANOVA values of response surface quadratic model for the flexural strength was shown in Table 5. The flexural strength model was significant because of the p-value ($P < 0.05$) with the t-test at a 5% level of significance. The F-value of 19.61 with a low probability value shows that the model was significant. The p-value of 0.2225, 0.1591, and 0.6288 for the flexural strength property indicates that A,AB, and B^2 are not significant while the other values are. The ANOVA results illustrated a reasonable confidence in the estimate of the flexural strength efficiency ($R^2 = 0.9334$). Also, the predicted R^2 was 0.4749, which is in agreement, within a reasonable limit, with the adjusted R^2 of 0.8858 for the flexural strength of LWAC as illustrated in Table 5. It is an acceptable adjustment as it is high and close to 1. The adequate precision value of 14.1457 for the flexural strength, which is more than 4, is satisfactory and validates the adopted model.

Fig. 13(b) shows the normal plots of the residual values of the flexural strength. For the model adequacy, the residuals from the ANOVA results are significant. The plot between the studentized flexural strength residuals and normal % of probability agreed with the straight line, hence, validating the model. On the other hand, the effects of the NPOFA and POC replacement levels on the flexural strength of LWAC are shown in the 2D and 3D surface response plots as illustrated in Fig. 14. It can be observed that the low flexural strength values are related with a high POC replacement level. The LWAC flexural strength reduced to 5.05 MPa with 100% replacement level of POC. Whereas, the NPOFA has a minor effect on the flexural strength.

4.3. Analysis of splitting tensile strength results

The combined effects of the NPOFA replacement level (%) (A) and POC replacement level (%) (B) on the improving of splitting tensile strength are described by the perturbation plots as illustrated in Fig. 15(a). The curvature (B) which represents the POC is certainly harsher than the curve (A), indicating that the splitting tensile strength is affected more by the POC replacement level in the LWAC mix. The splitting tensile strength of LWAC decreased when the POC replacement level increased. The empirical relationship between the factors (NPOFA and POC) and the splitting tensile strength (τ_{sp}) in terms of coded factors is given as in Eq. (4).

$$\tau_{sp} = 4.9 - 0.25A - 0.7433B - 0.015AB - 0.4345A^2 - 0.2345B^2 \quad (4)$$

The interactions between the factors significantly affected the splitting tensile strength. The ANOVA values of response surface quadratic model for the splitting tensile strength were shown in Table 5. The splitting tensile strength model was significant because of the p-value ($P < 0.05$) with the t-test at a 5% level of significance. The F-value of 24.78 with low probability value shows that the model was significant. The interactions between all factors are also significant. The ANOVA results illustrated a reliable confidence in the estimate of the splitting tensile strength efficiency ($R^2 = 0.9465$). The predicted R^2 of 0.5316 agrees, within a reasonable limit, with the adjusted R^2 of 0.9083. The adequate precision value of 16.4688 for the splitting tensile strength, which is more than 4, is satisfactory and confirms the validation of the predicted model.

Fig. 15(b) shows the normal plots of the residual values of the splitting tensile strength to evaluate the splitting tensile strength and

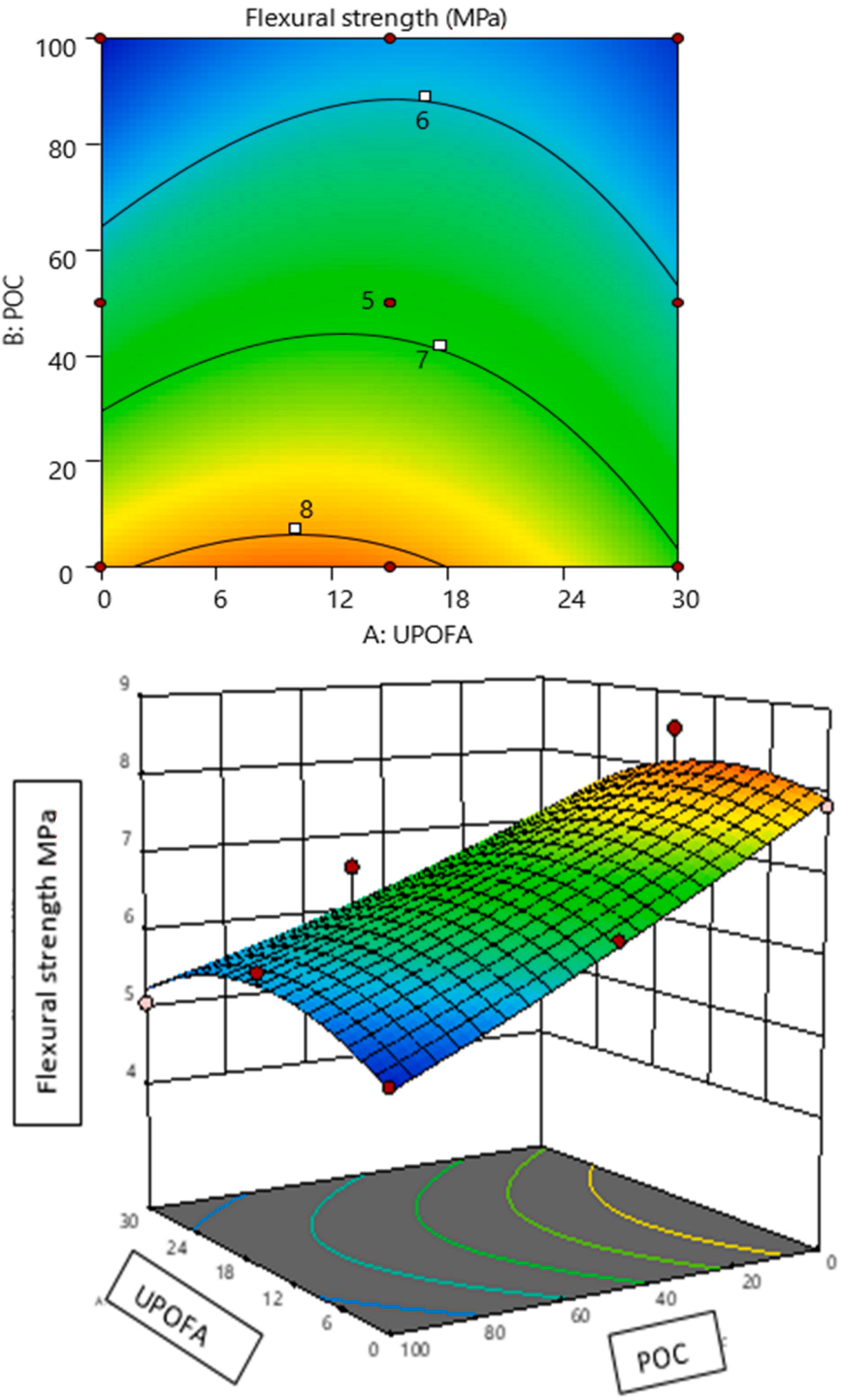

Fig. 14. The 2D and 3D surface response plots of flexural strength.

determine the model suitability. For the model adequacy, the residuals from the ANOVA results are significant. The plot between the studentized residuals of splitting tensile strength and normal % of probability agreed with the straight line, hence, validating the model. Subsequently, this model can be used to navigate the design space.

On the other hand, the effects of the NPOFA and POC replacement levels on the splitting tensile strength of LWAC performance are presented in the 2D and 3D surface response plots as illustrated in Fig. 16. It can be observed that the low splitting tensile strength values are related with a higher POC replacement level. When POC was increased as coarse aggregate, the LWAC splitting tensile

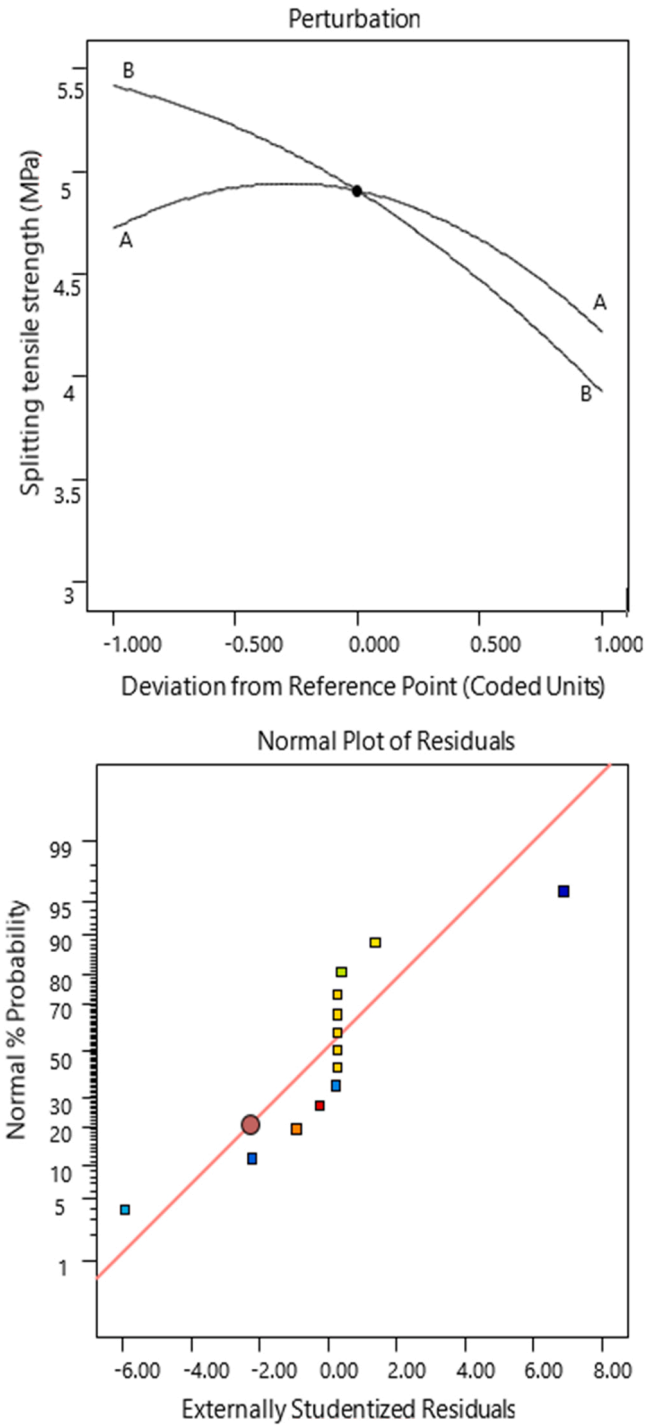

Fig. 15. Perturbation curve and normal plots of residual values of the tensile strength.

strength decreased to be 3.45 MPa with a 100% replacement level of POC.

5. Optimization of results

Optimization requires the simultaneous assessment of different responses. Therefore, to enhance the functional relationships between variables (factors) and the responses, the optimization analysis was conducted by the established mathematical model to get the optimal composition of NPOFA and POC. The optimization standards for UPV, flexural strength, and splitting tensile strength are

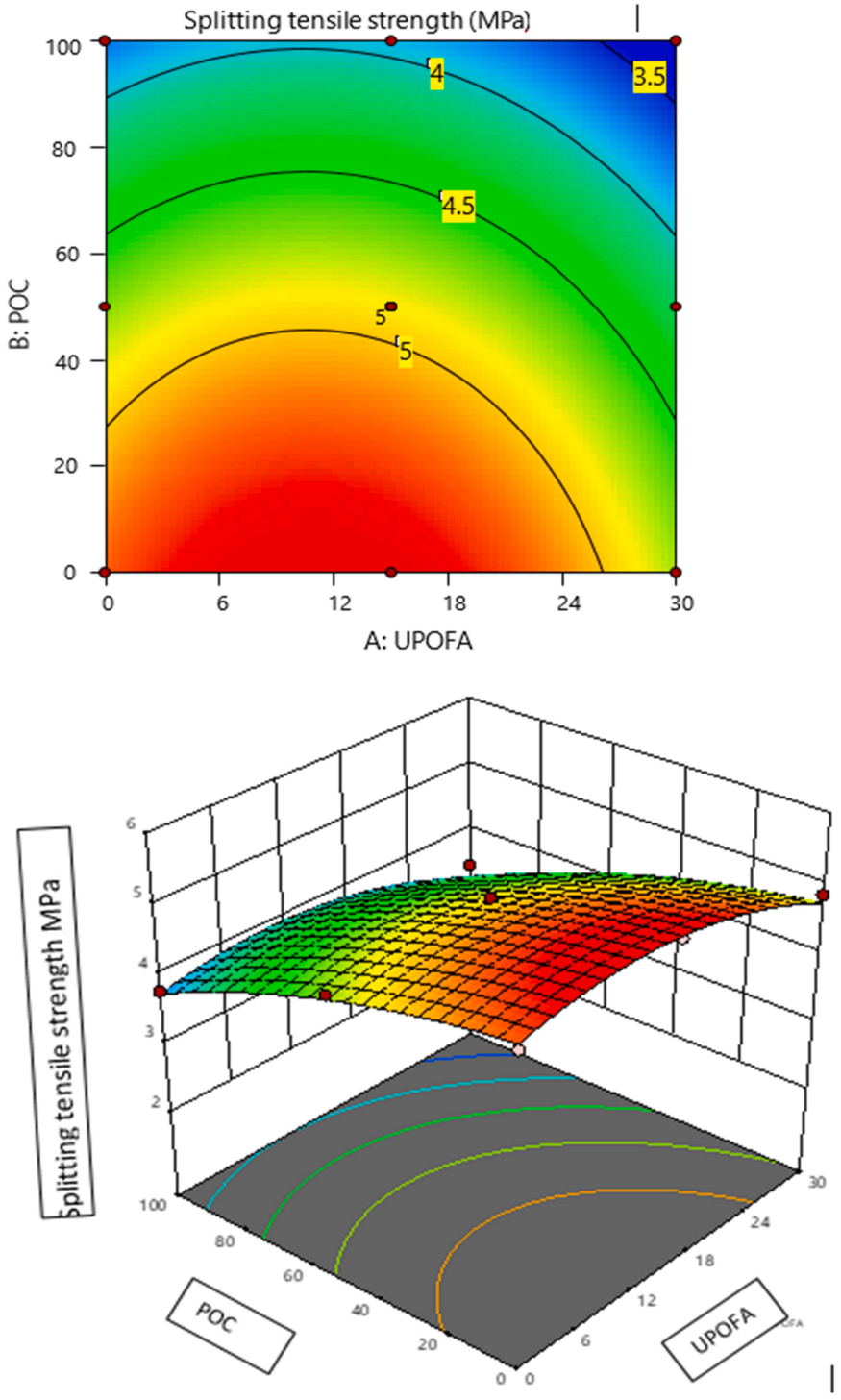

Fig. 16. The 2D and 3D surface response plots of splitting tensile strength.

shown in Table 6. The standards to complete the goal of the desired replacement of NPOFA and POC were targeted maximum UPV, maximum flexural strength, and maximum splitting tensile strength, at 360-day.

Numerical multi-objective optimization was utilized to find out the best quantity of NPOFA and POC, with maximizing the UPV, flexural, and tensile strengths of the LWAC. The focus of the optimization study was mainly on recognizing the desired values of independent variables to obtain optimization aims. The RSM technique was used to enhance the three responses as these were influenced by several variables. Table 7 summarizes the optimum solutions identified by the CCD within the RSM technique. The best

Table 6
Optimization standards of individual responses for LWAC.

Name	Goal	Lower Limit	Upper Limit	Importance
A:UPOFA	In range	0	30	3
B:POC	In range	0	100	3
UPV	maximize	3212	4375	5
Flexural strength	maximize	5.05	8.53	5
Tensile strength	maximize	3.45	5.38	5

Table 7
Optimum ratios and related predicted response.

Number	UPOFA	POC	UPV m/s	Flexural strength MPa	Splitting tensile strength Mpa	Desirability
1	5.331	0	4231.01	8.123	5.384	0.918
2	5.209	0	4232	8.12	5.381	0.918
3	5.438	0	4230.14	8.126	5.386	0.918
4	5.611	0	4228.73	8.13	5.39	0.918
5	5.793	0	4227.26	8.134	5.394	0.918
6	5.986	0	4225.69	8.138	5.397	0.918
7	6.852	0	4218.65	8.154	5.412	0.917
8	7.389	0	4214.29	8.162	5.42	0.917
9	9.763	0	4195.01	8.178	5.442	0.913
10	12.75	0	4170.75	8.155	5.438	0.903
11	0.598	0	4269.45	7.947	5.238	0.888
12	17.25	0	4134.2	8.03	5.368	0.877
13	20.25	0	4109.83	7.885	5.278	0.841

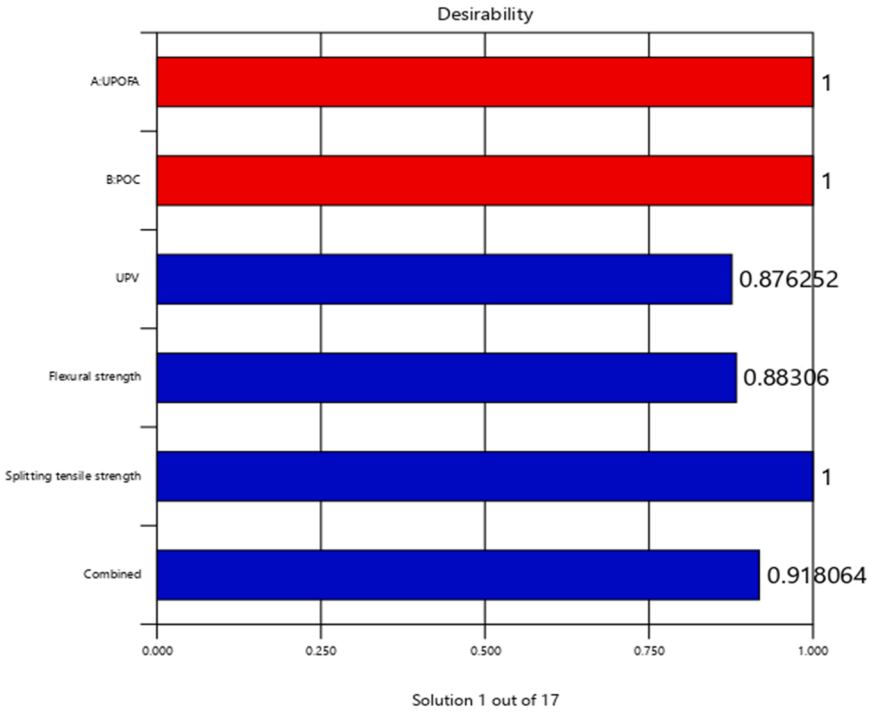

Fig. 17. Optimization solution 1 out of 17.

solution of desirability was for the tests 1–6 at 0.918. The aim of each optimization method was designed according to the weight or importance factor. The solution 1 out of 17 is given in Fig. 17.

In this research, all the responses were fixed with the same importance related to the aim because the concrete properties investigated refer to the concrete strength. Table 7 shows that the desirability ranged from 0.918 to 0.841 for the optimal solutions. 0% POC with a 5.209–20.25% NPOFA achieved these desirability values. The first six tests achieved the highest desirability of 0.918 with 0% POC and 5.331–5.986% NPOFA. These optimum values were predicted to achieve 4231.007–4225.685 m/s UPV, with

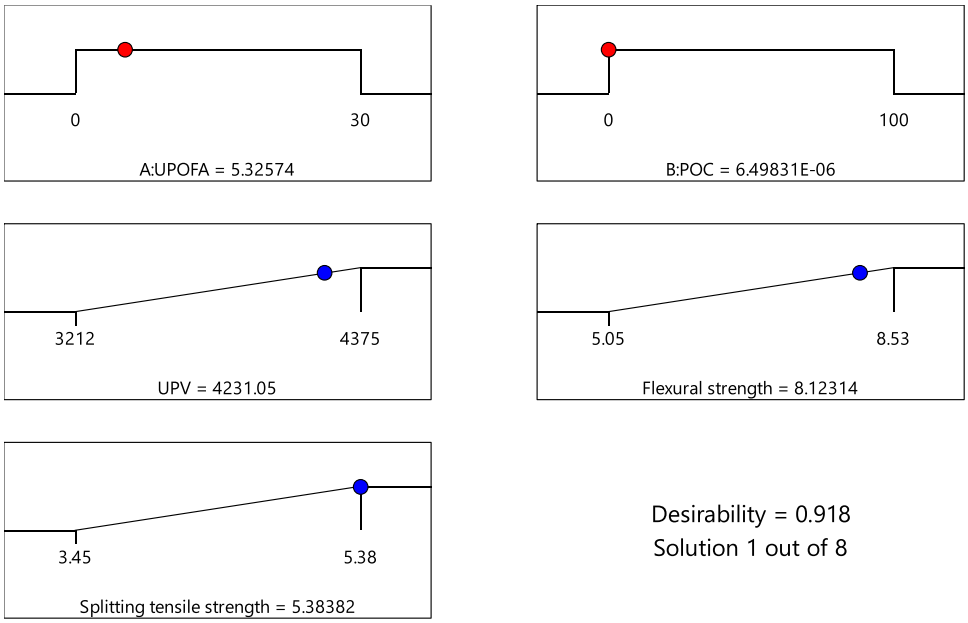

Fig. 18. Numerical optimization ramps with desirability 0.619 and solution 1 out of 2.

8.123–8.138 MPa as flexural strength, and 5.384–5.397 MPa as splitting tensile strength.

The graphical ramp for the optimized responses is shown in Fig. 18. It can be observed that the multi-objective optimization of results are 5.331% as replacement level of NPOFA and 2.408% as replacement level of POC aggregates. While, the optimum values of UPV, flexural strength, and splitting tensile strength are 4231 m/s, 8.123 MPa, and 5.383 MPa, respectively. In this research, all the responses (UPV, flexural strength, and splitting tensile strength) were identified with the same significance related to the study goal. The desirability of the optimal solutions was 0.918.

6. Conclusions

This study emphasizes on characterization and optimization of responses using RSM in LWAC. NPOFA was used as cement replacement from 0% to 30% and POC aggregate was used as partial/full replacement of coarse aggregate from 0% to 100% in producing LWAC. Based on the results obtained from this study, some conclusions were drawn as presented here:

1. The concrete strength recognized by the UPV, flexural and tensile strength demonstrated a growth with mix containing 15% NPOFA and 0% POC aggregate.
2. Higher replacement levels of POC aggregate led to a significant decrease in UPV, flexural and splitting tensile strengths. The decreasing values can be attributed to the physical properties of POC, such as the pore structure and high void content in its particles.
3. Incorporating Nano-POFA led to enhancing the concrete strength, especially at later curing ages. This enhancement in the strength was due to the high pozzolanic reaction that developed with time.
4. All concrete properties investigated have a good relationship between the variables (NPOFA and POC) on one side and their responses (UPV, flexural and tensile strengths) on the other side.
5. The results of the optimization used by RSM illustrates that the optimum strengths were gained by incorporating 5.331% NPOFA as cement replacement and 2.408% POC as coarse aggregate replacement.

For future studies, it is suggested to include other variables such as adopted different curing conditions, water cement ratio, and utilization of various volume fractions of steel fiber. Also, the concrete samples can be exposed to acid and sulfate environments in order to study their behavior when subjected to adverse environmental conditions.

Funding

We want to thank the University Malaysia Pahang, PGRS 180328 to support and assist us in our research.

Declaration of Competing Interest

The authors declare that they have no known competing financial interests or personal relationships that could have appeared to influence the work reported in this paper.

References

[1] J. Pirker, A. Mosnier, F. Kraxner, P. Havlík, M. Obersteiner, What are the limits to oil palm expansion? Glob. Environ. Chang. 40 (2016) 73–81.
[2] A.M. Zeyad, B.A. Tayeh, A.M. Saba, M. Johari, Workability, setting time and strength of high-strength concrete containing high volume of palm oil fuel ash, Open Civ. Eng. J. 12 (1) (2018).
[3] A.M. Zeyad, M.M. Johari, B.A. Tayeh, M.O. Yusuf, Efficiency of treated and untreated palm oil fuel ash as a supplementary binder on engineering and fluid transport properties of high-strength concrete, Constr. Build. Mater. 125 (2016) 1066–1079.
[4] H. Hamada, B. Tayeh, F. Yahaya, K. Muthusamy, A. Al-Attar, Effects of nano-palm oil fuel ash and nano-eggshell powder on concrete, Constr. Build. Mater. 261 (2020), 119790.
[5] M.T. Teguh, K. Anuar, M. Taslim, R.G. Saputra, The application of empty palm fruit bunch (EPFB) as a material for fixed wing type unmanned aerial vehicle fuselage production, J. Ocean Mech. Aerosp. Sci. Eng. 63 (3) (2019) 13–16.
[6] S. Zaini, C. Zheng, M. Abu, Costing structure improvement using activity based costing in palm oil plantation of Malaysia, J. Mod. Manuf. Syst. Technol. 4 (1) (2020) 95–109.
[7] R. Singh, M.H. Ibrahim, N. Esa, M. Iliyana, Composting of waste from palm oil mill: a sustainable waste management practice, Rev. Environ. Sci. Bio/Technol. 9 (4) (2010) 331–344.
[8] F.M. Said, N.F. Hamid, M.A.-A. Razali, N.F.S. Daud, S.M. Ahmad, Transformation Process of Agricultural Waste to Chemical Production via Solid-State Fermentation, Bio-valorization of Waste, Springer, 2021, pp. 187–201.
[9] M. Aslam, P. Shafigh, M.Z. Jumaat, M. Lachemi, Benefits of using blended waste coarse lightweight aggregates in structural lightweight aggregate concrete, J. Clean. Prod. 119 (2016) 108–117.
[10] B.S. Mohammed, M.A. Al-Ganad, M. Abdullahi, Analytical and experimental studies on composite slabs utilising palm oil clinker concrete, Constr. Build. Mater. 25 (8) (2011) 3550–3560.
[11] T. Hemalatha, M. Mapa, N. George, S. Sasmal, Physico-chemical and mechanical characterization of high volume fly ash incorporated and engineered cement system towards developing greener cement, J. Clean. Prod. 125 (2016) 268–281.
[12] E. Benhelal, G. Zahedi, E. Shamsaei, A. Bahadori, Global strategies and potentials to curb CO_2 emissions in cement industry, J. Clean. Prod. 51 (2013) 142–161.
[13] A. Tolstoy, V. Lesovik, E. Glagolev, A. Krymova, Synergetics of hardening construction systems, IOP Conf. Ser. Mater. Sci. Eng. (2018).
[14] H.M. Hamada, B.S. Thomas, B. Tayeh, F.M. Yahaya, K. Muthusamy, J. Yang, Use of oil palm shell as an aggregate in cement concrete: a review, Constr. Build. Mater. 265 (2020), 120357.
[15] H.M. Hamada, A. Alya'a, F.M. Yahaya, K. Muthusamy, B.A. Tayeh, A.M. Humada, Effect of high-volume ultrafine palm oil fuel ash on the engineering and transport properties of concrete, Case Stud. Constr. Mater. 12 (2020), e00318.
[16] H. Hamada, A. Alattar, F. Yahaya, K. Muthusamy, B.A. Tayeh, Mechanical properties of semi-lightweight concrete containing nano-palm oil clinker powder, Phys. Chem. Earth Parts A/B/C. 121 (2021), 102977.
[17] M. Amin, A.M. Zeyad, B.A. Tayeh, I.S. Agwa, Effects of nano cotton stalk and palm leaf ashes on ultrahigh-performance concrete properties incorporating recycled concrete aggregates, Constr. Build. Mater. 302 (2021), 124196.
[18] A.S. Faried, S.A. Mostafa, B.A. Tayeh, T.A. Tawfik, Mechanical and durability properties of ultra-high performance concrete incorporated with various nano waste materials under different curing conditions, J. Build. Eng. 43 (2021), 102569.
[19] M. Amin, A.M. Zeyad, B.A. Tayeh, I.S. Agwa, Effect of ferrosilicon and silica fume on mechanical, durability, and microstructure characteristics of ultra high-performance concrete, Constr. Build. Mater. 320 (2022), 126233.
[20] W.S. Alaloul, M.A. Musarat, S. Haruna, K. Law, B.A. Tayeh, W. Rafiq, S. Ayub, Mechanical properties of silica fume modified high-volume fly ash rubberized self-compacting concrete, Sustainability 13 (10) (2021) 5571.
[21] S.M. Qaidi, B.A. Tayeh, H.F. Isleem, A.R. de Azevedo, H.U. Ahmed, W. Emad, Sustainable utilization of red mud waste (bauxite residue) and slag for the production of geopolymer composites: a review, Case Stud. Constr. Mater. (2022), e00994.
[22] M.M. Ahmed, K. El-Naggar, D. Tarek, A. Ragab, H. Sameh, A.M. Zeyad, B.A. Tayeh, I.M. Maafa, A. Yousef, Fabrication of thermal insulation geopolymer bricks using ferrosilicon slag and alumina waste, Case Stud. Constr. Mater. 15 (2021), e00737.
[23] M. Amran, G. Murali, N.H.A. Khalid, R. Fediuk, T. Ozbakkaloglu, Y.H. Lee, S. Haruna, Y.Y. Lee, Slag uses in making an ecofriendly and sustainable concrete: a review, Constr. Build. Mater. 272 (2021), 121942.
[24] A. Ramezanianpour, V. Malhotra, Effect of curing on the compressive strength, resistance to chloride-ion penetration and porosity of concretes incorporating slag, fly ash or silica fume, Cem. Concr. Compos. 17 (2) (1995) 125–133.
[25] G. Li, X. Zhao, Properties of concrete incorporating fly ash and ground granulated blast-furnace slag, Cem. Concr. Compos. 25 (3) (2003) 293–299.
[26] B.A. Tayeh, M. Hadzima-Nyarko, A.M. Zeyad, S.Z. Al-Harazin, Properties and durability of concrete with olive waste ash as a partial cement replacement, Adv. Concr. Constr. 11 (1) (2021) 59–71.
[27] D. Tobbala, A. Rashed, B.A. Tayeh, T.I. Ahmed, Performance and microstructure analysis of high-strength concrete incorporated with nanoparticles subjected to high temperatures and actual fires, Arch. Civ. Mech. Eng. 22 (2) (2022) 1–15.
[28] A.M. Zeyad, M.A.M. Johari, A. Abutaleb, B.A. Tayeh, The effect of steam curing regimes on the chloride resistance and pore size of high–strength green concrete, Constr. Build. Mater. 280 (2021), 122409.
[29] A.M. Zeyad, M.A.M. Johari, Y.R. Alharbi, A.A. Abadel, Y.M. Amran, B.A. Tayeh, A. Abutaleb, Influence of steam curing regimes on the properties of ultrafine POFA-based high-strength green concrete, J. Build. Eng. 38 (2021), 102204.
[30] M.M. Johari, A. Zeyad, N.M. Bunnori, K. Ariffin, Engineering and transport properties of high-strength green concrete containing high volume of ultrafine palm oil fuel ash, Constr. Build. Mater. 30 (2012) 281–288.
[31] K.-H. Yang, J.-K. Song, K.-I. Song, Assessment of CO_2 reduction of alkali-activated concrete, J. Clean. Prod. 39 (2013) 265–272.
[32] G. Jokhio, H. Hamada, A. Humada, Y. Gul, A. Abu-Tair, Environmental benefits of incorporating palm oil fuel ash in cement concrete and cement mortar, E3S Web of Conferences, EDP Sciences, 2020, p. 03005.
[33] J.-H. Tay, Ash from oil-palm waste as a concrete material, J. Mater. Civ. Eng. 2 (2) (1990) 94–105.
[34] J.-H. Tay, K.-Y. Show, Use of ash derived from oil-palm waste incineration as a cement replacement material, Resour. Conserv. Recycl. 13 (1) (1995) 27–36.
[35] M. Safiuddin, M. Abdus Salam, M.Z. Jumaat, Utilization of palm oil fuel ash in concrete: a review, J. Civ. Eng. Manag. 17 (2) (2011) 234–247.
[36] H.M. Hamada, G.A. Jokhio, F.M. Yahaya, A.M. Humada, Y. Gul, The present state of the use of palm oil fuel ash (POFA) in concrete, Constr. Build. Mater. 175 (2018) 26–40.
[37] H.M. Hamada, F.M. Yahaya, K. Muthusamy, G.A. Jokhio, A.M. Humada, Fresh and hardened properties of palm oil clinker lightweight aggregate concrete incorporating Nano-palm oil fuel ash, Constr. Build. Mater. 214 (2019) 344–354.
[38] M.M.U. Islam, K.H. Mo, U.J. Alengaram, M.Z. Jumaat, Mechanical and fresh properties of sustainable oil palm shell lightweight concrete incorporating palm oil fuel ash, J. Clean. Prod. 115 (2016) 307–314.
[39] C. Jaturapitakkul, J. Tangpagasit, S. Songmue, K. Kiattikomol, Filler effect and pozzolanic reaction of ground palm oil fuel ash, Constr. Build. Mater. 25 (11) (2011) 4287–4293.

[40] N.H.A.S. Lim, M.A. Ismail, H.S. Lee, M.W. Hussin, A.R.M. Sam, M. Samadi, The effects of high volume nano palm oil fuel ash on microstructure properties and hydration temperature of mortar, Constr. Build. Mater. 93 (2015) 29–34.
[41] B. Alsubari, P. Shafigh, Z. Ibrahim, M.F. Alnahhal, M.Z. Jumaat, Properties of eco-friendly self-compacting concrete containing modified treated palm oil fuel ash, Constr. Build. Mater. 158 (2018) 742–754.
[42] A.N. Mohammed, M.A.M. Johari, A.M. Zeyad, B.A. Tayeh, M.O. Yusuf, Improving the engineering and fluid transport properties of ultra-high strength concrete utilizing ultrafine palm oil fuel ash, J. Adv. Concr. Technol. 12 (4) (2014) 127–137.
[43] M.A.A. Rajak, Z.A. Majid, M. Ismail, Morphological characteristics of hardened cement pastes incorporating nano-palm oil fuel ash, Procedia Manuf. 2 (2015) 512–518.
[44] M.W. Hussin, N.H.A.S. Lim, A.R.M. Sam, M. Samadi, M.A. Ismail, N.F. Ariffin, N.H.A. Khalid, M.Z.A. Majid, J. Mirza, H. Lateef, Long term studies on compressive strength of high volume nano palm oil fuel ash mortar mixes, J. Teknol. 77 (16) (2015).
[45] P. Chindaprasirt, S. Homwuttiwong, C. Jaturapitakkul, Strength and water permeability of concrete containing palm oil fuel ash and rice husk–bark ash, Constr. Build. Mater. 21 (7) (2007) 1492–1499.
[46] W. Kroehong, T. Sinsiri, C. Jaturapitakkul, Effect of palm oil fuel ash fineness on packing effect and pozzolanic reaction of blended cement paste, Procedia Eng. 14 (2011) 361–369.
[47] M.N. Huda, M.Z.B. Jumat, A.S. Islam, Flexural performance of reinforced oil palm shell & palm oil clinker concrete (PSCC) beam, Constr. Build. Mater. 127 (2016) 18–25.
[48] R. Ahmmad, M. Jumaat, S. Bahri, A.S. Islam, Ductility performance of lightweight concrete element containing massive palm shell clinker, Constr. Build. Mater. 63 (2014) 234–241.
[49] P. Shafigh, H.B. Mahmud, M.Z.B. Jumaat, R. Ahmmad, S. Bahri, Structural lightweight aggregate concrete using two types of waste from the palm oil industry as aggregate, J. Clean. Prod. 80 (2014) 187–196.
[50] K.H. Mo, U.J. Alengaram, M.Z. Jumaat, Compressive behaviour of lightweight oil palm shell concrete incorporating slag, Constr. Build. Mater. 94 (2015) 263–269.
[51] S.A. Kabir, U.J. Alengaram, M.Z. Jumaat, S. Yusoff, A. Sharmin, I.I. Bashar, Performance evaluation and some durability characteristics of environmental friendly palm oil clinker based geopolymer concrete, J. Clean. Prod. 161 (2017) 477–492.
[52] P. Owens, Lightweight aggregates for structural concrete. Structural Lightweight Aggregate Concrete, 1993, pp. 1–18.
[53] D.C.L. Teo, M.A. Mannan, V.J. Kurian, Structural concrete using oil palm shell (OPS) as lightweight aggregate, Turk. J. Eng. Environ. Sci. 30 (4) (2006) 251–257.
[54] D.C. Teo, M.A. Mannan, J.V. Kurian, Flexural behaviour of reinforced lightweight concrete beams made with oil palm shell (OPS), J. Adv. Concr. Technol. 4 (3) (2006) 459–468.
[55] D.C. Montgomery, Design and Analysis of Experiments, John Wiley & Sons, 2017.
[56] P.S. Lovato, E. Possan, D.C.C. Dal Molin, Â.B. Masuero, J.L.D. Ribeiro, Modeling of mechanical properties and durability of recycled aggregate concretes, Constr. Build. Mater. 26 (1) (2012) 437–447.
[57] A. Khodaii, H. Haghshenas, H.K. Tehrani, Effect of grading and lime content on HMA stripping using statistical methodology, Constr. Build. Mater. 34 (2012) 131–135.
[58] J.A. Cornell, A.I. Khuri, Response Surfaces: Designs and Analyses, Marcel Dekker, Inc., 1987.
[59] P. Nanthagopalan, M. Santhanam, Fresh and hardened properties of self-compacting concrete produced with manufactured sand, Cem. Concr. Compos. 33 (3) (2011) 353–358.
[60] C.-L. Hwang, L.A.-T. Bui, K.-L. Lin, C.-T. Lo, Manufacture and performance of lightweight aggregate from municipal solid waste incinerator fly ash and reservoir sediment for self-consolidating lightweight concrete, Cem. Concr. Compos. 34 (10) (2012) 1159–1166.
[61] A.A. Awal, H. Mohammadhosseini, Green concrete production incorporating waste carpet fiber and palm oil fuel ash, J. Clean. Prod. 137 (2016) 157–166.
[62] A.A. Awal, I. Shehu, M. Ismail, Effect of cooling regime on the residual performance of high-volume palm oil fuel ash concrete exposed to high temperatures, Constr. Build. Mater. 98 (2015) 875–883.
[63] F. Abutaha, H. Abdul Razak, J. Kanadasan, Effect of palm oil clinker (POC) aggregates on fresh and hardened properties of concrete, Constr. Build. Mater. 112 (2016) 416–423.
[64] M.Z. Jumaat, U.J. Alengaram, R. Ahmmad, S. Bahri, A.B.M.S. Islam, Characteristics of palm oil clinker as replacement for oil palm shell in lightweight concrete subjected to elevated temperature, Constr. Build. Mater. 101 (2015) 942–951.
[65] A. Neville, Properties of Concrete CTP-VVP, Malaysia, 2008.
[66] J. Kanadasan, H. Abdul Razak, Engineering and sustainability performance of self-compacting palm oil mill incinerated waste concrete, J. Clean. Prod. 89 (2015) 78–86.
[67] F. Abutaha, H.A. Razak, H.A. Ibrahim, H.H. Ghayeb, Adopting particle-packing method to develop high strength palm oil clinker concrete, Resour. Conserv. Recycl. 131 (2018) 247–258.
[68] V.C. Li, T. Horikoshi, A. Ogawa, S. Torigoe, T. Saito, Micromechanics-based durability study of polyvinyl alcohol-engineered cementitious composite, Mater. J. 101 (3) (2004) 242–248.
[69] H. Ahmad, M. Hilton, N. Mohd Noor, Physical Properties of Local Palm Oil Clinker and Fly Ash, 2007.
[70] U.J. Alengaram, B.A. Al Muhit, M.Z. bin Jumaat, M.L.Y. Jing, A comparison of the thermal conductivity of oil palm shell foamed concrete with conventional materials, Mater. Des. 51 (2013) 522–529.
[71] H. Mohammadhosseini, R. Alyousef, N.H.A.S. Lim, M.M. Tahir, H. Alabduljabbar, A.M. Mohamed, M. Samadi, Waste metalized film food packaging as low cost and ecofriendly fibrous materials in the production of sustainable and green concrete composites, J. Clean. Prod. 258 (2020), 120726.
[72] I.I. Bashar, U.J. Alengaram, M.Z. Jumaat, A. Islam, H. Santhi, A. Sharmin, Engineering properties and fracture behaviour of high volume palm oil fuel ash based fibre reinforced geopolymer concrete, Constr. Build. Mater. 111 (2016) 286–297.
[73] S.K. Lim, C.S. Tan, O.Y. Lim, Y.L. Lee, Fresh and hardened properties of lightweight foamed concrete with palm oil fuel ash as filler, Constr. Build. Mater. 46 (2013) 39–47.
[74] M. Aldahdooh, N.M. Bunnori, M.M. Johari, Influence of palm oil fuel ash on ultimate flexural and uniaxial tensile strength of green ultra-high performance fiber reinforced cementitious composites, Mater. Des. 54 (2014) 694–701 (1980-2015).
[75] R.R. Nayaka, U.J. Alengaram, M.Z. Jumaat, S.B. Yusoff, R. Ganasan, Performance evaluation of masonry grout containing high volume of palm oil industry by-products, J. Clean. Prod. 220 (2019) 1202–1214.
[76] M. Aslam, P. Shafigh, M. Alizadeh Nomeli, M. Zamin Jumaat, Manufacturing of high-strength lightweight aggregate concrete using blended coarse lightweight aggregates, J. Build. Eng. 13 (2017) 53–62.
[77] K. Muthusamy, J. Mirza, N.A. Zamri, M.W. Hussin, A.P.A. Majeed, A. Kusbiantoro, A.M.A. Budiea, Properties of high strength palm oil clinker lightweight concrete containing palm oil fuel ash in tropical climate, Constr. Build. Mater. 199 (2019) 163–177.
[78] R. Polat, R. Demirboğa, M.B. Karakoç, İ. Türkmen, The influence of lightweight aggregate on the physico-mechanical properties of concrete exposed to freeze–thaw cycles, Cold Reg. Sci. Technol. 60 (1) (2010) 51–56.
[79] W.N.F.W. Hassan, M.A. Ismail, H.-S. Lee, M.S. Meddah, J.K. Singh, M.W. Hussin, M. Ismail, Mixture optimization of high-strength blended concrete using central composite design, Constr. Build. Mater. 243 (2020), 118251.
[80] R. Ahmmad, U.J. Alengaram, M.Z. Jumaat, N.H.R. Sulong, M.O. Yusuf, M.A. Rehman, Feasibility study on the use of high volume palm oil clinker waste in environmental friendly lightweight concrete, Constr. Build. Mater. 135 (2017) 94–103.